Journal of Magnetic Resonance 213 (2011) 82–89

Contents lists available at SciVerse ScienceDirect

Journal of Magnetic Resonance

journal homepage: www.elsevier.com/locate/jmr

Residual dipolar coupling between quadrupolar nuclei under magic-angle spinning and double-rotation conditions

Frédéric A. Perras, David L. Bryce *

Department of Chemistry, Centre for Catalysis Research and Innovation, University of Ottawa, 10 Marie Curie Private, Ottawa, Ontario, Canada K1N 6N5

ARTICLE INFO

Article history:
Received 7 July 2011
Revised 27 August 2011
Available online 17 September 2011

Keywords:
DOR
Solid-state NMR
Residual dipolar coupling
Line shape simulations
Exact quadrupolar interaction

ABSTRACT

Residual dipolar couplings between spin-1/2 and quadrupolar nuclei are often observed and exploited in the magic-angle spinning (MAS) NMR spectra of spin-1/2 nuclei. These orientation-dependent splittings contain information on the dipolar interaction, which can be translated into structural information. The same type of splittings may also be observed for pairs of quadrupolar nuclei, although information is often difficult to extract from the quadrupolar-broadened lineshapes. Here, the complete theory for describing the dipolar coupling between two quadrupolar nuclei in the frequency domain by Hamiltonian diagonalization is given. The theory is developed under MAS and double-rotation (DOR) conditions, and is valid for any spin quantum numbers, quadrupolar coupling constants, asymmetry parameters, and tensor orientations at both nuclei. All terms in the dipolar Hamiltonian become partially secular and contribute to the NMR spectrum. The theory is validated using experimental ^{11}B and $^{35/37}$Cl NMR experiments carried out on powdered B-chlorocatecholborane, where both MAS and DOR are used to help separate effects of the quadrupolar interaction from those of the dipolar interaction. It is shown that the lineshapes are sensitive to the quadrupolar coupling constant of both nuclei and to the J coupling (including its sign). From these experiments, the dipolar coupling constant for a heteronuclear spin pair of quadrupolar nuclei may be obtained as well as the sign of the quadrupolar coupling constant of the perturbing nucleus; these are two parameters that are difficult to obtain experimentally otherwise.

1. Introduction

Many of the current efforts in solid-state NMR spectroscopy focus on what has come to be known as NMR crystallography: to obtain crystallographic information from SSNMR data [1]. Much work has been done to relate the chemical shift (CS) and electric field gradient (EFG) tensors to the local environment of the nucleus [2–5]; however, the most generally useful interaction is arguably the dipolar interaction [6]. Dipolar couplings can yield unambiguous structural information because the only variable which influences the dipolar coupling constant (R_{DD}) for a given spin pair is the motionally-averaged inverse cube of the internuclear distance ($r_{1,2}$): $R_{DD} = \left(\frac{\mu_0}{4\pi}\right)\left(\frac{\gamma_1\gamma_2\hbar}{2\pi}\right)\langle r_{1,2}^{-3}\rangle$. What is measured experimentally is the effective dipolar coupling constant ($R_{eff} = R_{DD} - \Delta J/3$), which takes into account the anisotropy of the J coupling tensor (ΔJ) [7]. While ΔJ can be comparable to R_{DD} for heavy nuclear spin pairs such as the ^{199}Hg–^{31}P and ^{195}Pt–^{31}P pairs [8–11], it remains true that R_{eff} is usually a very good approximation to R_{DD} for the majority of spin pairs studied in materials and biomolecules. By selectively measuring the dipolar coupling constants between different nuclei, all the necessary information for solving the structure is given in principle [5,12–14]. Many dipolar recoupling experiments have been developed to measure quantitative dipolar couplings between spin-1/2 nuclei under MAS [15–20], although the analogous recoupling experiments involving a single quadrupolar nucleus and a spin-1/2 nucleus have been mainly successful in giving qualitative information [21,22]. For cases where the quadrupolar interaction is small enough to perform MAS, rotational resonance or double-quantum correlations can be used to measure dipolar couplings between quadrupolar nuclei; however, this cannot be applied to most pairs of quadrupolar nuclei [23–26]. Unfortunately, there is no generally applicable way of measuring dipolar coupling constants for pairs of quadrupolar nuclei in powders where the quadrupolar interaction is large, as the powder line shapes can span several megahertz.

It was shown by Kundla and Alla that a residual orientation-dependent line splitting remained in the MAS NMR spectra of spin-1/2 nuclei that are dipolar coupled to a quadrupolar nucleus [27], as the quadrupolar interaction is not completely averaged by MAS [28]. It is possible, under favorable conditions, to extract the dipolar coupling constant between a spin-1/2 nucleus and a quadrupolar nucleus by fitting the MAS spectrum of the spin-1/2 nucleus [29–37]. Residual dipolar couplings (RDC) have often been exploited for the ^{13}C–^{14}N spin pair, which directly yields chemical

* Corresponding author. Fax: +1 613 562 5170.
E-mail address: dbryce@uottawa.ca (D.L. Bryce).

1090-7807/$ - see front matter © 2011 Elsevier Inc. All rights reserved.
doi:10.1016/j.jmr.2011.08.043

information in biomolecules such as the bond distance and the bonding environment of nitrogen because the ^{14}N quadrupolar coupling constant's (C_Q) sign and magnitude depend strongly on the nitrogen environment [31,38–41].

In theory, the same RDCs could be measured for pairs of quadrupolar nuclei but this is difficult in practice as the quadrupolar interaction often dwarfs the other interactions. It was shown that the *J* splittings [42] and residual dipolar splittings for half-integer quadrupolar nuclei can be separated from the second-order quadrupolar broadening with the use of multiple quantum MAS (MQMAS) [43–47] and satellite transition MAS (STMAS) [48,49], but crystallite specific intensity losses and the two dimensional nature of the experiment can render the fitting of the spectra difficult [45,46]. Double-rotation (DOR) NMR may offer benefits as, in principle, there are no site specific intensity losses, and the basic method is purely one-dimensional [50–53].

Here, we discuss the theory behind the origin of RDC between two quadrupolar nuclei under MAS and DOR conditions. Previous approaches were either only valid for small C_Q values or used lengthy density matrix calculations [45–47]. In the present case, only the quadrupolar interaction is calculated exactly and so only a 4×4 matrix needs to be solved for a pair of spin-3/2 nuclei instead of a 16×16 matrix as was done previously [46]. This theory is then validated through the successful simulation of ^{11}B and $^{35/37}$Cl SSNMR spectra acquired for B-chlorocatecholborane.

2. Theoretical background

Frydman and co-workers have derived an expression based on average Hamiltonian theory for calculating the frequency shifts (ν_S) for a nucleus, *S,* in the DOR NMR spectrum of a quadrupolar heteronuclear spin pair arising from the residual dipolar coupling [45]. Their approach is typically valid if the ratio C_Q^I/ν_0^I is small and if the EFG at the observed nucleus is negligible, as all dependencies on the observed nucleus' EFG are ignored. More generally, an approach which considers the quadrupolar effects completely is desirable.

The Zeeman–quadrupolar (ZQ) Hamiltonian can be described according to Man [54]. One of the more popular ways to describe the ZQ interaction exactly is to solve the spin-only Schrödinger equation as an eigenproblem [55–57,29], although other treatments have also been presented [58–60]. We have used the eigenproblem approach presently. Most of the literature to date has focused solely on the case of an axially symmetric EFG tensor [29,31]; here, we have implemented the complete theory for an arbitrary value of η_Q.

To calculate the frequency shifts in the NMR spectrum of the observed nucleus *S* associated with the dipolar interaction with *I*, the expectation value of the dipolar Hamiltonian is calculated. Even though it is theoretically sound to diagonalize the ZQ Hamiltonians of both nuclei independently so as to obtain their eigenvectors, usually that is unnecessary as the observed nucleus typically has a small quadrupolar interaction relative to the Zeeman interaction; otherwise MAS or DOR would be experimentally impractical. In that case, perturbation theory is sufficient to represent the observed nucleus and its eigenvectors can be calculated analytically using standard methods [31]. Thus, perturbation theory can be used to represent the observed nucleus, whereas an exact diagonalization can be used for the perturbing nucleus. In the case mentioned earlier, a perturbation treatment was used for the perturbing nucleus whereas the quadrupolar interaction of the observed nucleus had been neglected [53]. The latter will of course permit faster spectral simulations, although large deviations from experiment are expected when the quadrupolar interaction is large. With the present treatment, all that is necessary to simulate the NMR spectra for a stationary powder sample is then to calculate these frequency shifts and add them to the resonance frequencies as calculated without a dipolar interaction (i.e., quadrupolar interaction and chemical shift). In the general case, the dipolar tensor and both EFG tensors will not be coincident and so the different EFG and dipolar principal axis systems (PASs) need to be related to one another using Euler angles. In this work we have used the ZXZ convention [61].

In principle, for the case of two quadrupolar nuclei that are dipolar coupled to one another, three Euler angles are necessary to relate one of the generally asymmetric EFG PASs to the other (α_Q, β_Q, γ_Q), and another two Euler angles are necessary to bring the axially symmetric dipolar PAS into coincidence with the first EFG tensor (α_D, β_D). In theory there are then a maximum of eleven parameters that would affect the MAS NMR spectrum of one of the crystallographically non-equivalent quadrupolar nuclei that are dipolar coupled to one another, if *J* coupling is ignored ($\delta_{iso}, C_Q^I, C_Q^S, \eta_Q^I, \eta_Q^S, R_{eff}, \alpha_Q, \beta_Q, \gamma_Q, \alpha_D, \beta_D$). The EFG parameters for the perturbing nucleus may be obtained independently from a separate NMR experiment (or, e.g., NQR), assuming that its spectrum is negligibly affected by the dipolar interaction to the first nucleus. An independent DOR experiment may also be used to remove the second-order quadrupolar broadening in the spectrum of the observed nucleus so as to obtain the analogue of an MAS spectrum of a spin-1/2 nucleus dipolar coupled to a quadrupolar nucleus. Lastly, molecular or crystallographic symmetry restraints may reduce the number of possible Euler angle values, further helping to establish the spectral fitting parameters as unique.

In the present work, the effect of MAS has been introduced in the same way as done by Menger and Veeman [29], by assuming an infinite spin rate. In this situation, the MAS NMR spectrum of the spin *S* is composed of lines originating from the average of the crystallite orientations sampled during a rotor cycle [32]. DOR NMR spectra have been simulated in a similar way, although a double loop was implemented so as to average the resonances associated with the crystallite orientations for an inner rotor rotation with a fixed outer rotor angle. Under MAS, the frequency shifts associated with the dipolar interaction are composed of $2I + 1$ second-order line shapes. These line shapes have both an anisotropic component, which leads to the shape of the lines, and a dipolar-induced isotropic shift. The $\hat{A}$ term of the dipolar Hamiltonian is non-zero even for a pair of spin-1/2 nuclei although it is nearly completely averaged by MAS. The quadrupolar interaction of the perturbing nucleus reintroduces the effects of the $\hat{C}$ and $\hat{D}$ terms, as in the case of the spin-1/2 and quadrupolar nucleus spin pair. The quadrupolar interaction of the observed nucleus will contribute to the halves of the $\hat{C}$ and $\hat{D}$ terms, which are null in the spin-1/2 case, i.e., those including the ladder operators for the observed nucleus, and will reintroduce effects from the $\hat{B}$, $\hat{E}$, and $\hat{F}$ terms which are typically smaller in magnitude. For a homonuclear spin pair, the situation is slightly different as the $\hat{B}$ term becomes generally secular [45]. The same treatment as that described in this work may also be used for homonuclear spin pairs, but the "*S*" operators must be replaced by their "*I*" equivalent or vice versa.

Line shape simulations of the ^{11}B MAS dipole–dipole shifts were done for a fictitious ^{11}B and ^{35}Cl spin pair at 4.7 T having coincident, axial EFG tensors to see the effect of these additional terms which are neglected in typical treatments of RDC (Fig. 1). To demonstrate the effect of these terms, the ^{11}B second-order quadrupolar broadening was removed and only the dipolar broadening is shown. The C_Q of the chlorine site was fixed at −41 MHz, the dipolar coupling constant was 713 Hz and the C_Q of the boron-11 was incremented to demonstrate the effects of the additional terms that only contribute to the spectra when two quadrupolar nuclei are involved. The spectrum with a $C_Q(^{11}B)$ of 0 MHz is identical to the spin-1/2 case, although it can be seen that the line shapes,

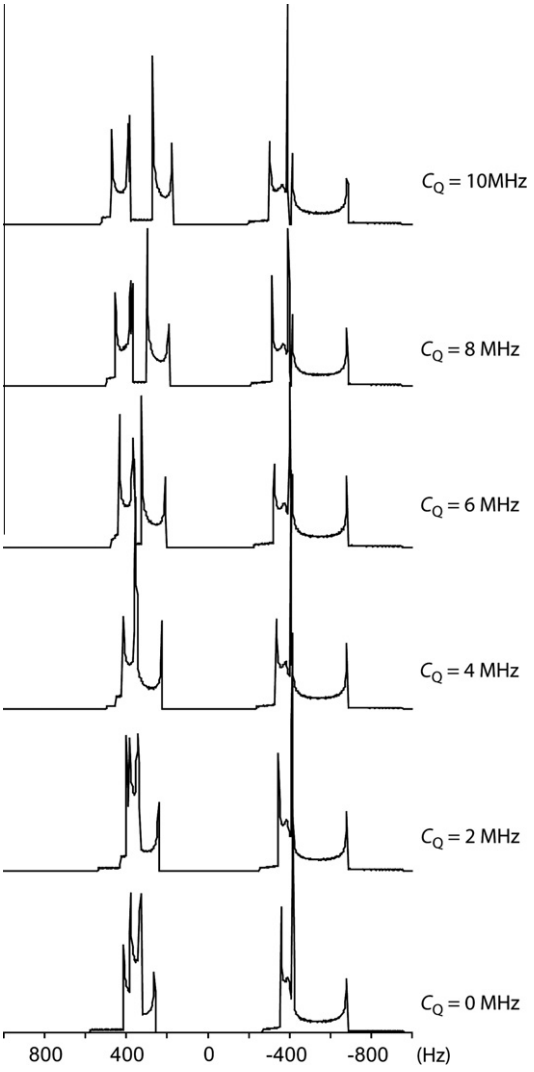

Fig. 1. Line shape simulations of the ^{11}B MAS dipolar splittings for a fictitious ^{11}B–^{35}Cl spin pair having a $C_Q(^{35}Cl)$ of −41 MHz, $\eta_Q(^{35}Cl)$ of 0, R_{eff} of 713 Hz and coincident dipolar and EFG tensor PASs at 4.7 T. The second-order ^{11}B quadrupolar broadening is removed to clearly show the effects of the dipolar splittings. The ^{11}B C_Q is increased stepwise to demonstrate the effects that the new secular terms of the dipolar interaction can have on the spectrum.

and the positions of the powder patterns, change drastically as the boron C_Q is increased. This effect may not be noticeable if the observed nucleus' C_Q is small.

In DOR, the orientationally dependent broadening caused by the chemical shift anisotropy, the quadrupolar interaction, and the dipolar interaction are completely averaged to their isotropic values. There remains, however, an isotropic dipolar shift which depends on the spin-state of the perturbing nucleus, and which is conceptually similar to the second-order quadrupole-induced shift [45,47,62]. The existence of these dipolar-induced shifts indicates that multiplets should also be observed in the DOR NMR spectra and that in general, each magnetically unique nuclear site is not represented by a single sharp resonance, as the resonance frequency will depend on the spin state of the perturbing nucleus, m_I.

Finally, second-order quadrupole effects need to be added to the expressions describing the MAS and DOR cases. In MAS this may be done simply by displacing the calculated dipolar frequencies by the chemical shift and the second-order resonance frequencies of a quadrupolar nucleus undergoing MAS. These may be calculated using the expressions derived by Kundla and co-workers

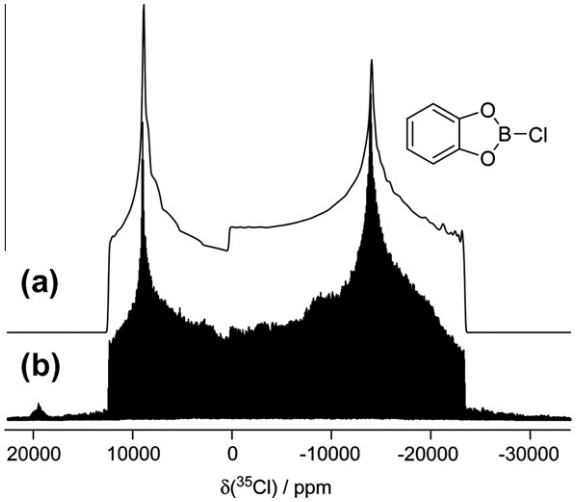

Fig. 2. Experimental (b) and simulated (a) ^{35}Cl WURST-QCPMG NMR spectra of B-chlorocatecholborane (**1**), the structure of which is shown in the upper right corner. Parameters are given in Table 1. B_0=21.1 T.

[63]. In the case of DOR, only the isotropic chemical shift and second-order quadrupole-induced shift need to be added to obtain the correct spectrum [64].

3. Results and discussion

As an experimental verification of this theory, B-chlorocatecholborane (**1**) (structure in Fig. 2) was chosen because of the potentially large $^{35/37}$Cl C_Q, the smaller ^{11}B C_Q, and the symmetry elements present in the molecule. The crystal structure has been solved by X-ray diffraction, according to which a static ^{35}Cl–^{11}B dipolar coupling constant of 713 Hz is to be expected [65]. There is a C_2 rotation axis along the chlorine–boron bond, which forces one principal component of both EFG tensors to be aligned along the bond.

To further reduce the number of fitting parameters required for the ^{11}B MAS and DOR NMR spectra (*vide infra*), ^{35}Cl and ^{37}Cl WURST-QCPMG [66] NMR spectra were acquired at 21.1 T (see Fig. 2; ^{37}Cl spectrum not shown) to independently measure the chlorine quadrupolar interaction parameters. From these, a $|C_Q(^{35}Cl)|$ of 41.9 ± 0.1 MHz was obtained along with an η_Q of 0.25 ± 0.03 and an isotropic chemical shift (δ_{iso}) of 50 ± 50 ppm. In this case, the small effects of dipolar coupling and chemical shift anisotropy were safely ignored as the dipolar coupling constant is only 713 Hz whereas the central transition powder pattern spans over 3 MHz. An upper limit for the span of the CS tensor of roughly 400 ppm can be estimated from the line shapes through simulations (not shown). Typical chlorine CS tensor spans are generally much less than 400 ppm [67]; gauge-including projector augmented wave (GIPAW) DFT calculations (*vide infra*) predict a chlorine CS tensor span of 246 ppm, which does not notably affect the line shape.

^{11}B DOR NMR spectra of **1** were acquired at 4.7 T (Fig. 3a) using rotor synchronized acquisition to remove half of the sidebands [68]. At this magnetic field, the quadrupolar interaction for chlorine cannot be well described by second-order perturbation theory (for ^{35}Cl, ν_Q/ν_0 = 1.16) and an exact description of the quadrupolar interaction must be applied to simulate the ^{11}B NMR spectrum, as presented above. For this reason the simulations in Fig. 1 are in fact not composed of the 1:1 doublets predicted by perturbation theory. A simulation using perturbation theory shows that the size of the splitting, as well as the intensities of the lines, are incorrect. By fitting the DOR spectrum using perturbation theory, the magnitude of the chlorine C_Q would be predicted as 36 MHz. The true C_Q

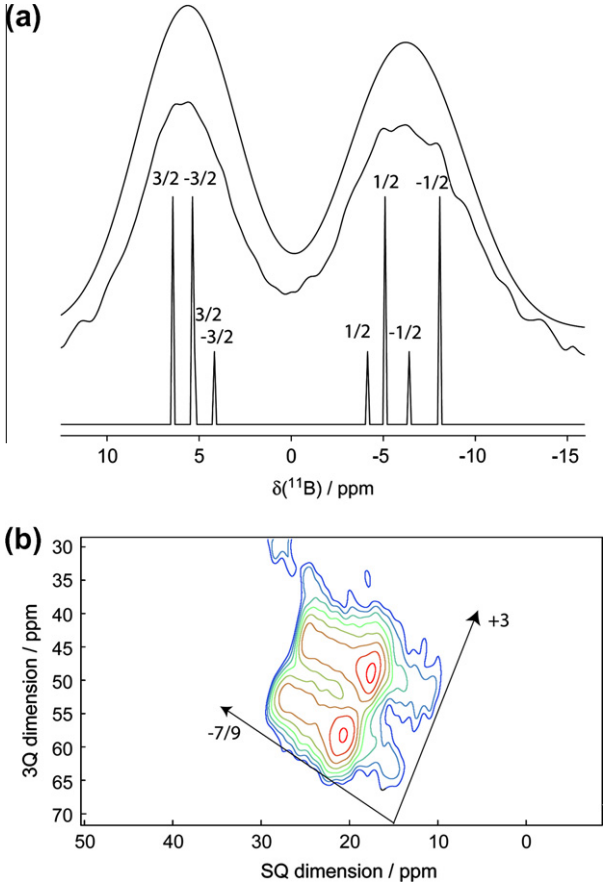

Fig. 3. (a) Experimental and simulated ^{11}B synchronized DOR centerbands for B-chlorocatecholborane at 4.7 T; the sidebands have been co-added into the centerband. The bottom trace shows the simulation without any line broadening of the eight resonances arising from the coupling to the four m_I states of ^{35}Cl (more intense lines) and ^{37}Cl (less intense lines). The m_I states to which these lines are attributed are annotated on the spectrum. The top trace includes 400 Hz of Lorentzian broadening. (b) ^{11}B MQMAS NMR spectrum of **1** acquired at 9.4 T. Arrows have been inserted to indicate the pseudo-isotropic axis (−7/9) as well as the RDC axis (+3).

of 41.9 MHz would then have been underestimated by 14%. The actual spectrum is composed of eight peaks, shown in the bottom trace of Fig. 3a, which correspond to the ^{11}B nucleus coupled to the four separate m_I levels of both ^{35}Cl and ^{37}Cl (natural abundances of 75.76% and 24.24%, respectively). The fit as presented incorporates the ^{35}Cl and ^{37}Cl NMR parameters determined independently, and the dipolar coupling constant calculated from the crystal structure (note that the ratio of quadrupole moments $Q(^{37}\text{Cl})/Q(^{35}\text{Cl})$ is 0.788 and the ratio of magnetogyric ratios $\gamma(^{37}\text{Cl})/\gamma(^{35}\text{Cl})$ is 0.832). The $^{35/37}$Cl quadrupolar coupling constants are negative, as surmised from the broader low-frequency peak in the DOR spectrum (the residual splitting is larger for those spin states (see Fig. 3a)). From the DOR spectrum, the sign of C_Q^I has thus been determined to be negative, something that cannot be easily obtained experimentally otherwise. The fact that one may obtain the sign of C_Q through dipolar coupling was noted by Casabella [69]. (It is important to note that the high frequency peak can be made broader in the simulations with the introduction of a large isotropic J coupling constant, although in that case the MAS spectra (*vide infra*) could no longer be fit.) A ^{11}B MQMAS spectrum of **1** provides further evidence that this splitting originates from residual dipolar coupling, as the slope along the dimension which separates the two patterns is +3, in agreement with the work of Wimperis and coworkers [44] (see Fig. 3b).

As discussed earlier, the quadrupolar interaction of the ^{11}B may also be important as the theory predicts that it affects the splitting observed in the DOR NMR spectrum. We therefore obtained the ^{11}B MAS NMR spectra of **1** at four applied magnetic field strengths (Fig. 4). The line shapes obtained have a large residual dipolar effect and we were only able to fit them using the theory discussed in this paper. The best fits of the spectra are given in Fig. 4 and the fitting parameters are listed in Table 1. These fits were done using coincident chlorine EFG and dipolar PASs (i.e., V_{33} and D_{33} lie along the same direction), although an Euler angle, β_Q, of 90° relating the boron EFG to the chlorine EFG was necessary. Due to the symmetry of the molecule, this angle can only take the values 0° or 90°. A comparison of the simulated spectra with a β_Q of 0° and 90° are shown in Fig. 4b. It can be seen that when the two EFGs are coincident ($\beta_Q = 0°$), the low frequency discontinuity at 9.4 T and 11.7 T is shifted to lower frequency. It is also seen that when γ_Q takes a value of 90°, the powder pattern is skewed to higher frequency, which is inconsistent with the experimental data.

From these simulations, it was then possible to obtain the ^{11}B quadrupolar interaction tensor parameters, as well as the relative orientation of the ^{11}B and $^{35/37}$Cl EFG tensors. The ^{11}B quadrupolar parameters agree with those inferred from independent ^{10}B NMR studies (not shown). The possibility of $^1J(^{35/37}\text{Cl}, ^{11}\text{B})$ coupling affecting the spectra was also investigated. The anisotropy of the J coupling tensor (ΔJ) is included as a negligible part of the effective dipolar coupling constant ($(\Delta J/3)/R_{\text{eff}} \approx 2\%$ according to quantum chemical calculations, *vide infra*), whereas the isotropic J coupling (J_{iso}) must be considered separately, as a part of the coupling Hamiltonian as follows (considering only the secular part), $\hat{H}_{D+J} = J_{\text{iso}}\hat{S}_Z\hat{I}_Z + \hat{H}_D$. This effect simply induces a shift in the position of the various MAS subspectra. As these are already separated independently by the dipolar interaction, the effect of the sign of J_{iso} will also be important. Additional simulations show that, in this case, a positive value of $^1J(^{35/37}\text{Cl}, ^{11}\text{B})_{\text{iso}}$ shifts the positions of the discontinuities mostly towards low frequency, whereas the intensity of the discontinuity at −4.5 ppm decreases drastically if J_{iso} is negative. In our case, the best fits of the five ^{11}B NMR spectra are with an isotropic ^{11}B–$^{35/37}$Cl J coupling constant of −30 ± 15 Hz.

As a final verification of our results, the experimental data are compared with the values calculated using PAW DFT [70–72]. This method uses a plane wave basis set with periodic boundary conditions in order to simulate a complete lattice and uses pseudopotentials for speed. The calculated EFG tensor parameters and chemical shifts are given in Table 1. These agree very well with experiment, although the ^{11}B C_Q is slightly overestimated. These calculations also provide some insight into the tensor orientations within the molecule frame. The chlorine EFG, in fact, shares the same PAS as the dipolar tensor and the largest principal component of the boron EFG (V_{33}) is perpendicular to the bond (i.e., $\beta_Q = 90°$), while V_{11} orients parallel to the B–Cl bond ($\alpha_Q = \gamma_Q = 0°$). This shows that these calculations are able to reproduce fairly well the EFG tensor magnitudes for boron and chlorine as well as the tensor orientations. It was also possible to confirm the experimentally-determined negative sign of the chlorine C_Q using these calculations.

J coupling tensor calculations were performed using the Amsterdam Density Functional software (ADF) [73–75]. Scalar and spin–orbit relativistic effects were included using the zeroth-order regular approximation (ZORA) [76,77]. These calculations predict a small and negative $^1J(^{35}\text{Cl}, ^{11}\text{B})_{\text{iso}}$ of −17.7 Hz and a $\Delta^1J(^{35}\text{Cl}, ^{11}\text{B})$ of 56.5 Hz. The computed value of $^1J(^{35}\text{Cl}, ^{11}\text{B})_{\text{iso}}$ is in agreement with experiment. The effect of the calculated ΔJ on the NMR spectra is in fact negligible, as shown through additional spectral simulations, and, it is therefore not possible to obtain this parameter from our simulations for this compound due to the large $R_{DD}/\Delta J$ ratio of ~12.6.

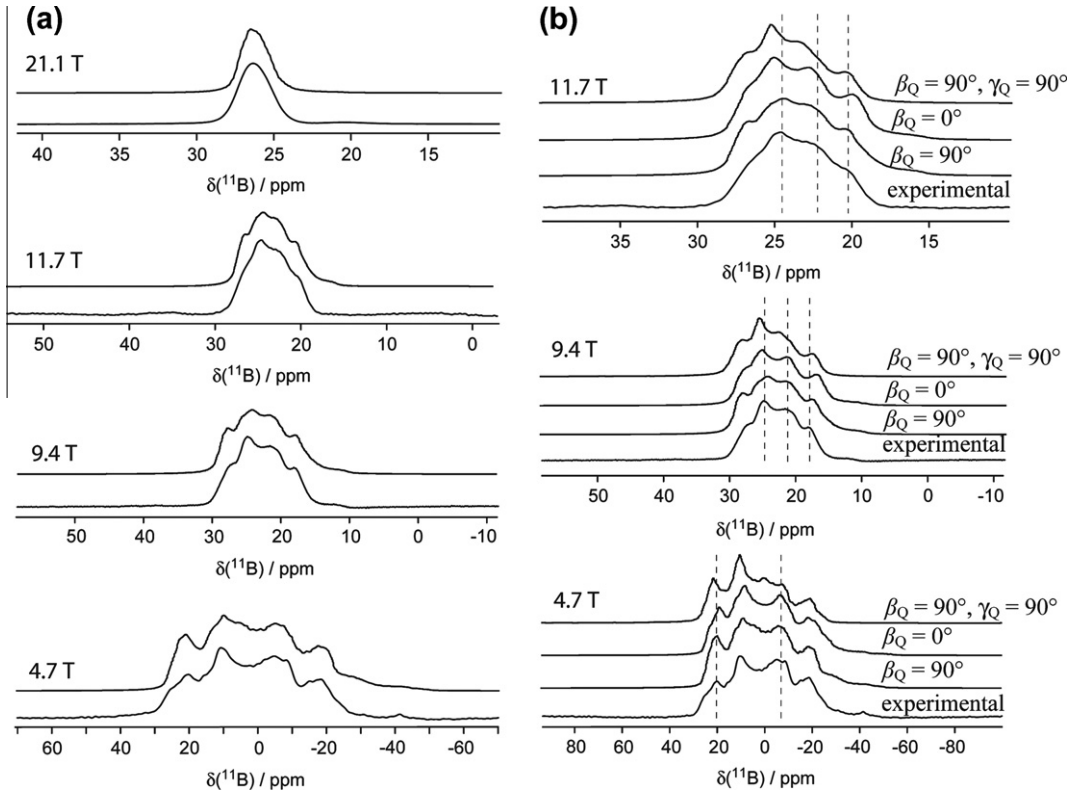

Fig. 4. (a) Experimental (bottom traces) and simulated (top traces) ^{11}B MAS NMR spectra of **1** at four applied magnetic fields. The simulations were performed using the parameters listed in Table 1. (b) Comparison of the ^{11}B MAS NMR spectral simulations having coincident EFG tensors ($\beta_Q = 0°$) or perpendicular V_{33} principal components ($\beta_Q = 90°$). The best fits are deemed to be those where $\beta_Q = 90°$. Simulations are also shown when γ_Q is equal to 90°.

Table 1
Experimental and calculated NMR parameters for **1.**

Parameter	Experimental	Calculated
δ_{iso}(Cl)	50 ± 50 ppm	120 ppm[a]
$C_Q(^{35}Cl)$	−41.9 ± 0.1 MHz	−41.3 MHz
$\eta_Q(^{35}Cl)$	0.25 ± 0.03	0.27
δ_{iso}(B)	28 ± 1 ppm	44.6 ppm[b]
$\lvert C_Q(^{11}B)\rvert$	2.1 ± 0.1 MHz	2.4 MHz
$\eta_Q(^{11}B)$	0.15 ± 0.05	0.15
α_Q	0°[d]	3.9°
β_Q	90°	90°
γ_Q	0°	0°
R_{DD}	713 Hz	713 Hz
β_D	0°	0°
$J(^{35}Cl, ^{11}B)_{iso}$	−30 ± 15 Hz	−17.7 Hz
$\Delta J(^{35}Cl, ^{11}B)$	n/a	56.5 Hz
η_J[c]	n/a	0.22

[a] Calculated using the absolute shielding of infinitely dilute Cl^- (σ_{iso} = 975 ppm) [82].
[b] Calculated using the absolute shielding of BF_3OEt_2 (σ_{iso} = 110.9 ppm) [83].
[c] η_J is the asymmetry parameter of the J coupling tensor ($J_{22} - J_{11}/J_{33} - J_{iso}$) where $|J_{33} - J_{iso}| \geqslant |J_{11} - J_{iso}| \geqslant |J_{22} - J_{iso}|$.
[d] The simulated spectra are not particularly sensitive to the value of α_Q due to the small value of $\eta_Q(^{11}B)$; however, the best fits were obtained with 0°.

4. Conclusion

The effects of residual dipolar coupling that are frequently seen in the MAS NMR spectra of spin-1/2 nuclei may also be observed in the MAS and DOR NMR spectra of quadrupolar nuclei. It has been shown that the quadrupolar effects of the observed nucleus and of the coupled nucleus need to be considered in order to reproduce the experimental lineshapes. This means that for a pair of quadrupolar nuclei, all terms in the dipolar Hamiltonian have nonzero secular parts that need to be included in the spectral simulations. A numerical treatment based on Menger and Veeman's original theory for residual dipolar coupling which has been extended to include the effects of non-zero η_Q, as well as the effect of the quadrupolar interaction at the observed nucleus, has been described.

The spectra are sensitive to the relative orientations of the two EFG tensors and the dipolar coupling tensor. The relative orientations of the EFG tensors obtained from experiment are in agreement with those predicted by PAW DFT calculations. From the DOR spectra at low field, it is also possible to obtain the sign of the quadrupolar coupling constant of the perturbing nucleus, a parameter that cannot be obtained by traditional experimental techniques. Spectral simulations also show that the lineshapes are sensitive to the sign of the J coupling constant as well and that a $^1J(^{35}Cl, ^{11}B)_{iso}$ of −30 ± 15 Hz was necessary to reproduce the experiment. The spectral splittings could also be used to measure dipolar coupling constants between quadrupolar nuclei, therefore yielding some structural information that can be difficult to obtain quantitatively with recoupling methods. Lastly, it is important to note that the number of resonances obtained in the DOR spectra of half-integer quadrupolar nuclei does not always reflect the number of sites in the crystal structure, and appropriate caution should be taken in the interpretation of such spectra.

5. Experimental

B-chlorocatecholborane (**1**) (97%) was purchased from Sigma–Aldrich and was tightly packed into the appropriate rotor under an inert atmosphere.

The $^{35/37}$Cl WURST-QCPMG spectra were acquired using the Bruker AVANCE II 900 spectrometer operating at 21.1 T ($\nu_0(^{35}Cl)$ = 88.2 MHz, $\nu_0(^{37}Cl)$ = 73.4 MHz) at the National Ultrahigh-Field NMR Facility for Solids in Ottawa using a double-resonance, 7 mm, static probe. Chemical shifts were referenced

to infinitely dilute Cl^- using NH_4Cl as a secondary reference (δ_{iso} = 73.8 ppm). For ^{35}Cl, a 50 μs WURST shape sweeping 2 MHz was used; a total of 96 echoes where collected while proton decoupling; a recycle delay of 0.5 s and a spikelet separation of 5 kHz were used. Variable offset cumulative spectrum (VOCS) acquisition methods were also necessary [78]. Seven spectra, each taking 2048 scans, were acquired with a frequency step of 500 kHz. In the case of ^{37}Cl NMR, a 50 μs WURST shape sweeping 1 MHz was used. In this case the VOCS frequency steps were 400 kHz and 3072 scans were acquired for each piece.

The ^{11}B DOR NMR spectrum was acquired using a Bruker AVANCE III 200 (4.7 T) spectrometer operating at 64.2 MHz for ^{11}B using a Bruker HP WB 73A DOR probe with a 4.3 mm inner rotor and a 14 mm outer rotor. The outer rotor spinning frequency was set at 910 Hz and synchronized acquisition was used to remove half of the sidebands [68]; a total of 432 scans were collected with a recycle delay of 2 s and a 4 μs central-transition selective pulse.

The ^{11}B MAS spectra were acquired using Bruker AVANCE II 900 (21.1 T), Bruker AVANCE 500 (11.7 T), Bruker AVANCE III 400 (9.4 T), and Bruker AVANCE III 200 (4.7 T)spectrometers. Either a Hahn-echo (21.1 T) or a one-pulse acquisition (11.7 T, 9.4 T, and 4.7 T) was used. The central-transition selective 90° pulse lengths were of 5 μs, 1.5 μs, 1 μs and 1.6 μs at 21.1 T, 11.7 T, 9.4 T and 4.7 T respectively. In all cases a 4 mm triple resonance MAS probe was used with a spin rate of 12 kHz. All ^{11}B NMR experiments were referenced to liquid $F_3B{\cdot}O(C_2H_5)_2$ using $NaBH_4$ as a secondary reference (δ_{iso} = −42.06 ppm).

The ^{11}B MQMAS spectrum of **1** was acquired at 9.4 T using the standard three pulse z-filtered sequence [79]. The excitation, conversion, and central transition selective pulses were 4.5 μs, 1.5 μs, and 19 μs respectively. Sixty transients were collected in each of the 26 t_1 increments. The t_1 increments were of 100 μs in order to synchronize t_1 with the MAS rate of 10 kHz.

The $^{35/37}Cl$ NMR spectra were fit using second-order perturbation theory as implemented in WSolids1 [80]. The ^{11}B MAS and DOR spectra were fit using an in-house simulation program written in C. This program diagonalizes the Zeeman–quadrupolar Hamiltonian for ^{35}Cl and ^{37}Cl sequentially. The dipolar shifts are calculated as described in this paper. Twenty three different crystallite orientations were considered for the MAS averaging whereas 90,000 (300 about both rotor axes) were used for DOR; no powder averaging was used for DOR.

The PAW DFT (GIPAW for the shielding calculations) calculations were done using the CASTEP program [70–72]. The generalized gradient approximation (GGA) of Perdew, Burke, and Ernzerhof (PBE) [81] was used along with on-the-fly generation pseudopotentials. The positions of the hydrogen atoms were first optimized with a kinetic energy cutoff of 450 eV; the NMR calculation then used a kinetic energy cutoff of 610 eV. A 4 × 4 × 4 k-point grid was used for all calculations. The isotropic magnetic shielding constants were converted to chemical shifts using the absolute shielding scales for chlorine [82] and boron [83].

The ZORA DFT calculations were performed using the CPL program [84–87] of ADF [73–75] using the linear density approximation of Vosko et al. [88] along with the hybrid GGA functional PBE0 [89]. The ZORA quadruple-zeta quadruple-polarized basis set (ZORA/QZ4P) was used for all atoms. The use of the jcpl basis set for chlorine yielded very similar results. The model for the ADF calculations was composed of a single molecule of **1**.

Acknowledgments

F.A.P. is grateful to the Natural Sciences and Engineering Research Council (NSERC) of Canada for a graduate scholarship. D.L.B. thanks NSERC, the Canada Foundation for Innovation, and the Ontario Ministry of Research and Innovation for funding. We thank Dr. Klaus Eichele and Dr. Gang Wu for helpful comments, and Dr. Henry J. Stronks and co-workers for supporting our DOR research program. Dr. Victor Terskikh, Dr. Eric Ye, and Dr. Glenn Facey are thanked for technical support. Access to the 900 MHz NMR spectrometer was provided by the National Ultrahigh-Field NMR Facility for Solids (Ottawa, Canada), a national research facility funded by the Canada Foundation for Innovation, the Ontario Innovation Trust, Recherche Québec, the National Research Council Canada, and Bruker BioSpin and managed by the University of Ottawa (www.nmr900.ca). NSERC is acknowledged for a Major Resources Support grant.

References

[1] R.K. Harris, R.E. Wasylishen, M.J. Duer, NMR crystallography, Wiley, Chichester, 2009.
[2] C.M. Widdifield, D.L. Bryce, Crystallographic structure refinement with quadrupolar nuclei: a combined solid-state NMR and GIPAW DFT example using $MgBr_2$, Phys. Chem. Chem. Phys. 11 (2009) 7120–7122.
[3] D.H. Brouwer, G.D. Enright, Probing local structure in zeolite frameworks: ultrahigh-field NMR measurements and accurate first-principles calculations of zeolite ^{29}Si magnetic shielding tensors, J. Am. Chem. Soc. 130 (2008) 3095–3105.
[4] B. Zhou, T. Giavani, H. Bildsøe, J. Skibsted, H.J. Jakobsen, Structure refinement of $CsNO_3$(II) by Coupling of ^{14}N MAS NMR experiments with WIEN2k DFT calculations, Chem. Phys. Lett. 402 (2005) 133–137.
[5] E. Salager, R.S. Stein, C.J. Pickard, B. Elena, L. Emsley, Powder NMR crystallography of thymol, Phys. Chem. Chem. Phys. 11 (2009) 2610–2621.
[6] G.E. Pake, Nuclear resonance absorption in hydrated crystals: fine structure of the proton line, J. Chem. Phys. 16 (1948) 327–336.
[7] This expression assumes that the dipolar and **J** tensors share the same PAS and that **J** is axially symmetric.
[8] J. Vaara, J. Jokisaari, R.E. Wasylishen, D.L. Bryce, Spin-spin coupling tensors as determined by experiment and computational chemistry, Prog. Nucl. Magn. Reson. Spectrosc. 41 (2002) 233–304.
[9] D.L. Bryce, N.M.D. Courchesne, F.A. Perras, Measurement of $\Delta^1J(^{199}Hg,^{31}P)$ in $[HgPCy_3(OAc)_2]_2$ and relativistic ZORA DFT investigations of mercury-phosphorus coupling tensors, Solid State Nucl. Magn. Reson. 36 (2009) 182–191.
[10] W.P. Power, R.E. Wasylishen, Anisotropies of the ^{31}P chemical shift and ^{31}P–^{195}Pt indirect spin–spin coupling in platinum(II) phosphines, Inorg. Chem. 31 (1992) 2176–2183.
[11] M.D. Lumsden, K. Eichele, R.E. Wasylishen, T.S. Cameron, J.F. Britten, Determination of a ^{199}Hg–^{31}P indirect spin–spin coupling tensor via single-crystal phosphorus NMR spectroscopy, J. Am. Chem. Soc. 116 (1994) 11129–11136.
[12] B. Elena, G. Pintacuda, N. Mifsud, L. Emsley, Molecular structure determination in powders by NMR crystallography from proton spin diffusion, J. Am. Chem. Soc. 128 (2006) 9555–9560.
[13] D.H. Brouwer, NMR crystallography of zeolites: refinement of an NMR-solved crystal structure using ab initio calculations of ^{29}Si chemical shift tensors, J. Am. Chem. Soc. 130 (2008) 6306–6307.
[14] D.H. Brouwer, R.J. Darton, R.E. Morris, M.H. Levitt, A solid-state NMR method for solution of zeolite crystal structures, J. Am. Chem. Soc. 127 (2005) 10365–10370.
[15] R. Tycko, G. Dabbagh, Measurement of nuclear magnetic dipole–dipole couplings in magic angle spinning NMR, Chem. Phys. Lett. 173 (1990) 461–465.
[16] B.-Q. Sun, P.R. Costa, D. Kocisko, P.T. Lansbury Jr., R.G. Griffin, Internuclear distance measurements in solid state nuclear magnetic resonance: dipolar recoupling via rotor synchronized spin locking, J. Chem. Phys. 102 (1995) 702–707.
[17] D.K. Sodickson, M.H. Levitt, S. Vega, R.G. Griffin, Broad band dipolar recoupling in the nuclear magnetic resonance of rotating solids, J. Chem. Phys. 98 (1993) 6742–6748.
[18] S.E. Shore, J.-P. Ansermet, C.P. Slichter, J.H. Sinfelt, Nuclear-magnetic-resonance study of the bonding and diffusion of CO chemisorbed on Pd, Phys. Rev. Lett. 58 (1987) 953–956.
[19] T. Gullion, J. Schaefer, Rotational-echo double-resonance NMR, J. Magn. Reson. 81 (1989) 196–200.
[20] I. Schnell, H.W. Spiess, High-resolution ^1H NMR spectroscopy in the solid state: very fast sample rotation and multiple-quantum coherences, J. Magn. Reson. 151 (2001) 153–227.
[21] T. Gullion, Measurement of dipolar interactions between spin-1/2 and quadrupolar nuclei by rotational-echo adiabatic-passage double-resonance NMR, Chem. Phys. Lett. 246 (1995) 325–330.
[22] C.P. Grey, W.S. Veeman, The detection of weak heteronuclear coupling between spin 1 and spin 1/2 nuclei in MAS NMR; $^{14}N/^{13}C/^1H$ triple resonance experiments, Chem. Phys. Lett. 192 (1992) 379–385.
[23] M. Nijman, M. Ernst, A.P.M. Kentgens, B.H. Meier, Rotational-resonance NMR experiments in half-integer quadrupolar spin systems, Mol. Phys. 98 (2000) 161–178.

[24] G. Mali, G. Fink, F. Taulelle, Double-quantum homonuclear correlation magic angle sample spinning nuclear magnetic resonance spectroscopy of dipolar-coupled quadrupolar nuclei, J. Chem. Phys. 120 (2004) 2835–2845.

[25] A. Brinkmann, A.P.M. Kentgens, T. Anupõld, A. Samoson, Symmetry-based recoupling in double-rotation NMR spectroscopy, J. Chem. Phys. 129 (2008) 174507.

[26] S. Wi, J.W. Logan, D. Sakellariou, J.D. Walls, A. Pines, Rotary resonance recoupling for half-integer quadrupolar nuclei in solid-state nuclear magnetic resonance spectroscopy, J. Chem. Phys. 117 (2002) 7024–7033.

[27] E. Kundla, M. Alla, Line splittings through dipole-dipole interaction with quadrupole nuclei in high resolution NMR powder spectra, in: E. Kundla, E. Lippmaa, T. Saluvere (Eds.), Proc. Cong. Ampere 20th, Springer-Verlag, Berlin, Heidelberg, New York, 1979. p. 92.

[28] S.N. Stuart, Residual interactions of a quadrupolar nucleus subject to high magnetic field and magic-angle spinning, Solid State Nucl. Magn. Reson. 3 (1994) 199–207.

[29] E.M. Menger, W.S. Veeman, Quadrupole effects in high-resolution phosphorus-31 solid-state NMR spectra of triphenylphosphine copper(I) complexes, J. Magn. Reson. 46 (1982) 257–268.

[30] A.C. Olivieri, How to write a program to simulate solid-state NMR line shapes, Concepts Magn. Reson. 8 (1996) 279–292.

[31] R.K. Harris, A.C. Olivieri, Quadrupolar effects transferred to spin-1/2 magic-angle spinning spectra of solids, Prog. Nucl. Magn. Reson. Spectrosc. 24 (1992) 435–456.

[32] S.H. Alarcón, A.C. Olivieri, R.K. Harris, Quadrupole effects of spin-3/2 nuclei on the solid-state magic-angle spinning nuclear magnetic resonance spectra of spin-1/2 nuclei, Solid State Nucl. Magn. Reson. 2 (1993) 325–334.

[33] J. Böhm, D. Fenzke, H. Pfeifer, Effects of quadrupolar nuclei on NMR spectra of $I = 1/2$ nuclei in magic-angle spinning experiments, J. Magn. Reson. 55 (1983) 197–204.

[34] N. Zumbulyadis, P.M. Henrichs, R.H. Young, Quadrupole effects in the magic-angle-spinning spectra of spin-1/2 nuclei, J. Chem. Phys. 75 (1981) 1603–1611.

[35] A.C. Olivieri, Quadrupolar effects in the CPMAS NMR spectra of spin-1/2 nuclei, J. Magn. Reson. 81 (1989) 201–205.

[36] D.L. VanderHart, H.S. Gutowsky, T.C. Farrar, Dipole–dipole interactions of a spin-1/2 nucleus with a quadrupole-coupled nucleus, J. Am. Chem. Soc. 89 (1967) 5056–5057.

[37] G. Wu, R.E. Wasylishen, The influence of the heteronuclear dipolar interaction on nuclear magnetic resonance spectra of quadrupolar nuclei, Mol. Phys. 95 (1998) 1177–1183.

[38] J.G. Hexem, M.H. Frey, S.J. Opella, Molecular and structural information from ^{14}N–^{13}C dipolar couplings manifested in high resolution ^{13}C NMR spectra of solids, J. Chem. Phys. 77 (1982) 3847–3856.

[39] A. Naito, S. Ganapathy, C.A. McDowell, High resolution solid state ^{13}C NMR spectra of carbons bonded to nitrogen in a sample spinning at the magic angle, J. Chem. Phys. 74 (1981) 5393–5397.

[40] A.C. Olivieri, L. Frydman, L.E. Diaz, A Simple approach for relating molecular and structural information to the dipolar coupling ^{13}C–^{14}N in CPMAS NMR, J.Magn. Reson. 75 (1987) 50–62.

[41] S. Wi, H. Sun, E. Oldfield, M. Hong, Solid-state NMR and quantum chemical investigations of $^{13}C^{\alpha}$ shielding tensor magnitudes and orientations in peptides: determining φ and ψ torsion angles, J. Am. Chem. Soc. 127 (2005) 6451–6458.

[42] G. Wu, S. Kroeker, R.E. Wasylishen, R.G. Griffin, Indirect spin–spin coupling in multiple-quantum magic-angle-spinning NMR spectra of quadrupolar nuclei, J. Magn. Reson. 124 (1997) 237–239.

[43] G. Wu, K. Yamada, Residual dipolar couplings in MAS and MQMAS NMR spectra of quadrupolar nuclei, Chem. Phys. Lett. 313 (1999) 519–524.

[44] J. McManus, R. Kemp-Harper, S. Wimperis, Second-order quadrupolar-dipolar broadening in two-dimensional multiple-quantum MAS NMR, Chem. Phys. Lett. 311 (1999) 292–298.

[45] S. Wi, L. Frydman, Residual dipolar couplings between quadrupolar nuclei in high resolution solid state NMR: description and observations in the high-field limit, J. Chem. Phys. 112 (2000) 3248–3261.

[46] S. Wi, V. Frydman, L. Frydman, Residual dipolar couplings between quadrupolar nuclei in solid state nuclear magnetic resonance at arbitrary fields, J. Chem. Phys. 114 (2001) 8511–8519.

[47] S.E. Ashbrook, J. McManus, M.J. Thrippleton, S. Wimperis, Second-order cross-term interactions in high-resolution MAS NMR of quadrupolar nuclei, Prog. Nucl. Magn. Reson. Spectrosc. 55 (2009) 160–181.

[48] S.E. Ashbrook, S. Wimperis, High-resolution NMR of quadrupolar nuclei in solids: the satellite-transition magic angle spinning (STMAS) experiment, Prog. Nucl. Magn. Reson. Spectrosc. 45 (2004) 53–108.

[49] S. Wi, S.E. Ashbrook, S. Wimperis, L. Frydman, Second-order quadrupole-shielding effects in magic-angle spinning solid-state nuclear magnetic resonance, J. Chem. Phys. 118 (2003) 3131–3140.

[50] A. Samoson, E. Lippmaa, A. Pines, High-resolution solid-state N.M.R. Averaging of second-order effects by means of a double-rotor, Mol. Phys. 65 (1988) 1013–1018.

[51] B.F. Chmelka, K.T. Mueller, A. Pines, J. Stebbins, Y. Wu, J.W. Zwanziger, Oxygen-17 NMR in solids by dynamic-angle spinning and double rotation, Nature 339 (1989) 42–43.

[52] A. Samoson, A. Pines, Double rotor for solid-state NMR, Rev. Sci. Instrum. 60 (1989) 3239–3241.

[53] Y. Wu, B.Q. Sun, A. Pines, A. Samoson, E. Lippmaa, NMR experiments with a new double rotor, J. Magn. Reson. 89 (1990) 297–309.

[54] P.P. Man, Quadrupolar interactions, in: D.M. Grant, R.K. Harris (Eds.), Encyclopedia of nuclear magnetic resonance, Wiley, Chichester, 1996, pp. 3838–3846.

[55] R.B. Creel, E. von Meerwall, C.F. Griffin, R.G. Barnes, NMR in the quadrupolar regime: chemical shifts, asymmetry parameter, and angular orientation, J. Chem. Phys. 58 (1973) 4930–4935.

[56] G.M. Muha, Exact solution of the eigenvalue problem for a spin 3/2 system in the presence of a magnetic field, J. Magn. Reson. 53 (1983) 85–102.

[57] R. Tycko, S.J. Opella, Overtone NMR spectroscopy, J. Chem. Phys. 86 (1987) 1761–1774.

[58] R.B. Creel, D.A. Drabold, Exact analytic solution of the spin 3/2 combined Zeeman–quadrupole hamiltonian, J. Mol. Struct. 111 (1983) 85–90.

[59] B.C. Sanctuary, T.K. Halstead, P.A. Osment, Multipole N.M.R. IV. Dynamics of single spins, Mol. Phys. 49 (1983) 753–784.

[60] A.D. Bain, Exact Calculation, using angular momentum, of combined Zeeman and quadrupolar interactions in NMR, Mol. Phys. 101 (2003) 3163–3175.

[61] W.P. Power, R.E. Wasylishen, S. Mooibroek, B.A. Pettitt, W. Danchura, Simulation of NMR powder line shapes of quadrupolar nuclei with half-integer spin at low-symmetry sites, J. Phys. Chem. 94 (1990) 591–598.

[62] Z. Gan, D.M. Grant, Molecular and structural information from variable-angle spinning NMR dipolar spectra of ^{13}C–^{14}N systems, J. Magn. Reson. 90 (1990) 522–534.

[63] E. Kundla, A. Samoson, E. Lippmaa, High-resolution NMR of quadrupolar nuclei in rotating solids, Chem. Phys. Lett. 83 (1981) 229–232.

[64] K.J.D. Mackenzie, M.E. Smith, Multinuclear solid-state NMR of inorganic materials, Elsevier Science, Oxford, 2002. pp. 68.

[65] R.B. Coapes, F.E.S. Souza, M.A. Fox, A.S. Batsanov, A.E. Goeta, D.S. Yufit, M.A. Leech, J.A.K. Howard, A.J. Scott, W. Clegg, T.B. Marder, Phosphine promoted substituent redistribution reactions of B-chlorocatechol borane: molecular structures of ClBcat BrBcat and L·ClBcat(cat = 1,2-$O_2C_6H_4$; L = PMe_3, PEt_3, PBu^t_3, PCy_3, NEt_3), J. Chem. Soc., Dalton Trans. (2001) 1201–1209.

[66] L.A. O'Dell, R.W. Schurko, QCPMG using adiabatic pulses for faster acquisition of ultra-wideline NMR spectra, Chem. Phys. Lett. 464 (2008) 97–102.

[67] R.P. Chapman, C.M. Widdifield, D.L. Bryce, Solid-state NMR of quadrupolar halogen nuclei, Prog. Nucl. Magn. Reson. Spectrosc. 55 (2009) 215–237.

[68] A. Samoson, E. Lippmaa, Synchronized double-rotation NMR spectroscopy, J. Magn. Reson. 84 (1989) 410–416.

[69] P.A. Casabella, Nuclear magnetic-dipole coupling in solid BF_3, J. Chem. Phys. 41 (1964) 3793–3798.

[70] M.D. Segall, P.J.D. Lindan, M.J. Probert, C.J. Pickard, P.J. Hasnip, S.J. Clark, M.C. Payne, First-principles simulation: ideas, illustrations and the CASTEP code, J. Phys.: Condens. Matter 14 (2002) 2717–2744.

[71] C.J. Pickard, F. Mauri, All-electron magnetic response with pseudopotentials: NMR chemical shifts, Phys. Rev. B 63 (2001) 245101.

[72] M. Profeta, F. Mauri, C.J. Pickard, Accurate first principles prediction of ^{17}O NMR parameters in SiO_2: assignment of the zeolite ferrierite spectrum, J. Am. Chem. Soc. 125 (2003) 541–548.

[73] G. te Velde, F.M. Bickelhaupt, E.J. Baerends, C. Fonseca Guerra, S.J.A. van Gisbergen, J.G. Snijders, T. Ziegler, Chemistry with ADF, J. Comput. Chem. 22 (2001) 931–967.

[74] C. Fonseca Guerra, J.G. Snijders, G. te Velde, E.J. Baerends, Towards an order-*N* DFT method, Theor. Chem. Acc. 99 (1998) 391–403.

[75] Amsterdam Density Functional Software ADF2009.01, SCM; Theoretical Chemistry, Vrije Universiteit: Amsterdam, The Netherlands, 2010. <http://www.scm.com/>.

[76] P. Pyykkö, Relativistic theory of nuclear spin–spin coupling in molecules, Chem. Phys. 22 (1977) 289–296.

[77] J. Autschbach, Two-component relativistic hybrid density functional computations of nuclear spin–spin coupling tensors using Slater-type basis sets and density-fitting techniques, J. Chem. Phys. 129 (2008) 094105.

[78] D. Massiot, I. Farnan, N. Gautier, D. Trumeau, A. Trokiner, J.P. Coutures, ^{71}Ga and ^{69}Ga nuclear magnetic resonance study of β-Ga_2O_3: resolution of four- and six-fold coordinated Ga sites in static conditions, Solid State Nucl. Magn. Reson. 4 (1995) 241–248.

[79] J.-P. Amoureux, C. Fernandez, S. Steuernagel, Z filtering in MQMAS NMR, J. Magn. Reson. Ser. A 123 (1996) 116–118.

[80] K. Eichele, R.E. Wasylishen, WSolids1: Solid-State NMR Spectrum Simulation Package, v. 1.19.11, University of Tübingen, Tübingen, Germany, 2009.

[81] J.P. Perdew, K. Burke, M. Ernzerhof, Generalized gradient approximation made simple, Phys. Rev. Lett. 77 (1996) 3865–3868.

[82] M. Gee, R.E. Wasylishen, A. Laaksonen, A more reliable absolute shielding scale for chlorine: combined experimental and theoretical approach, J. Phys. Chem. A 103 (1999) 10805–10812.

[83] K. Jackowski, W. Makulski, A. Szyprowska, A. Antušek, M. Jaszuński, J. Jusélius, NMR shielding constants in BF_3 and magnetic dipole moments of ^{11}B and ^{10}B nuclei, J. Chem. Phys. 130 (2009) 044309.

[84] J. Autschbach, T. Ziegler, Nuclear spin–spin coupling constants from regular approximate relativistic density functional calculations. I. Formalism and scalar relativistic results for heavy metal compounds, J. Chem. Phys. 113 (2000) 936–947.

[85] J. Autschbach, T. Ziegler, Nuclear spin–spin coupling constants from regular approximate relativistic density functional calculations. II. Spin–orbit coupling effects and anisotropies, J. Chem. Phys. 113 (2000) 9410–9418.

[86] R.M. Dickson, T. Ziegler, NMR spin–spin coupling constants from density functional theory with Slater-type basis functions, J. Phys. Chem. 100 (1996) 5286–5290.
[87] J. Khandogin, T. Ziegler, A density functional study of nuclear magnetic resonance spin-spin coupling constants in transition-metal systems, Spectrochim. Acta Part A 55 (1999) 607–624.
[88] S.H. Vosko, L. Wilk, M. Nusair, Accurate spin-dependent electron liquid correlation energies for local spin density calculations: a critical analysis, Can. J. Phys. 58 (1980) 1200–1211.
[89] C. Adamo, V. Barone, Toward reliable density functional methods without adjustable parameters: the PBE0 model, J. Chem. Phys. 110 (1999) 6158–6170.